https://doi.org/10.22226/2410-3535-2022-2-153-157

Microstructure of a titanium sample produced by ultrasonic consolidation

A. A. Mukhametgalina†, M. A. Murzinova, A. A. Nazarov

†a.mukhametgalina@mail.ru

Institute for Metals Superplasticity Problems, RAS, Ufa, 450001, Russia

The structure of a sample obtained by layer-by-layer consolidation of four sheets of commercially pure titanium with the thickness of 0.2 mm by means of ultrasonic welding was examined. It was shown that with each subsequent layer, the quality of the joints decreased. The formation of a joint of satisfactory quality was accompanied by a change in the microtexture, weak grain growth and the formation of a subgrain structure in the welded sheets, as well as an increase in microhardness in the joint zone by 30%.

Keywords: ultrasonic consolidation, commercially pure titanium, microstructure.

1. Introduction

Recently, additive manufacturing (AM) processes have been in the frontier of materials science and technology, because they allow one to enhance greatly the flexibility of production of three-dimensional parts and structures by a gradual, layer-by-layer build-up of material and reduce significantly the production waste [1–3]. There are many processes of AM of metallic materials [3], but directed energy deposition and powder bed fusion methods are currently the most used ones [4, 5]. Both of these processes are based on the depositing of the metal in the form of a powder or wire and melting it by a laser or electron beam and require an inert atmosphere or vacuum and careful temperature control.

One of the promising methods to form 3D as-built parts is ultrasonic additive manufacturing (UAM), which is based on the process of layer-by-layer ultrasonic welding of foils or sheets [6–11]. During UAM process, a specially designed sonotrode of an ultrasonic vibration system transmits the vibrations to a metal foil/sheet under the action of a clamping force, resulting in interfacial friction and plastic deformation between the substrate and the foil/sheet to be attached to achieve metallurgical bonding [7]. One of the main distinctions of UAM over other AM technologies is low heat generation, which results in the solid-state character of bonding, i. e. no melting of the metals occurs. Also, the generation of high residual stresses, dimensional changes of the 3D parts obtained are avoided in UAM process [8,11]. Additional advantages of UAM are the absence of gas shielding requirements, powder handling requirements, and high-power laser requirements [9]. UAM processes are not yet developed completely, but they were successfully used to consolidate soft materials, such as Al-based and Cu-based alloys [8–11]. Data concerning the ultrasonic consolidation of harder materials including titanium and its alloys are limited [12].

In our recent work [13], the regimes of spot ultrasonic welding of commercially pure Ti sheets with a thickness of 0.5 mm were determined and defect-free titanium joints with high strength were processed. Since UAM is based on ultrasonic welding (USW), the UAM process may be physically simulated by layer-by-layer USW using, for instance, an ultrasonic spot welding machine. In the present paper, this approach was used for ultrasonic consolidation of titanium sheets and examination of the structure and microhardness of the consolidated sample.

2. Materials and methods

Annealed sheets of commercially pure titanium (CP Ti) with the thickness of 0.2 mm were taken as a material for the study. Cards with sizes 10×20 mm were cut out from the sheet. The surfaces to be joined were ground sequentially using P40 and P220 abrasive papers, then washed with isopropyl alcohol and dried. An experimental home-made USW setup described in [14,15] was used for ultrasonic consolidation of the CP Ti cards. Four cards were jointed together layer by layer with ultrasonic vibrations with a frequency of 20 kHz and amplitude of 20 μm under the clamping force of 6 kN during 2 s. The welding tip with dimensions of 5×6 mm having a serrated surface comprised of eleven parallel teeth vibrated in the plane of the sheets parallel to the rolling direction.

The macro- and microstructure examination carried out in a cross section of the consolidated sample. Plane of the section passed through the center of the weld spot parallel to the direction of vibrations. The surfaces of the sections were ground and mechanically polished with 0.05 μm colloidal suspension of silicon oxide. The structure was studied by scanning electron microscopy on a TESCAN MIRA 3 LMH FEG microscope equipped with back-scattered electron (BSE) and electron backscatter diffraction (EBSD) detectors and Channel 5 software.

Data collection for EBSD analyses was performed with scan step of 1 μm. EBSD maps, 200 μm in width and 300 μm

in height, were obtained from each weld joint that made it possible to obtain a qualitative and quantitative information on the structure over the entire height of the cross section of the consolidated sample. The quality of the maps was considered satisfactory if the number of indexed points (with mean angular deviation less than 1°) were more than 80%. It should be noted that most of unindexed points (zero solutions) were located in the joint zones (near contact surfaces of the joined sheets). To avoid errors during the noise reduction (i. e. "replacing" voids and gaps with indexing points), the noise reduction procedure was stopped, if the minimum number of indexed neighbors around the "zero solution" was six (out of eight possible).

When analyzing the EBSD data, boundaries with misorientations from 2 to 15° were considered as low angle boundaries (LABs) and those with misorientations more than 15° were considered as high angle boundaries (HABs). A fragment with an area of at least 5 points was taken as a grain. The equivalent diameter was taken as the grain size. Quantitative analysis of the microstructure was performed in accordance with the requirements of ASTM E112-10.

The Vickers microhardness was measured using an ITV-1-AM testing instrument with a load on the indenter of 10 g and an exposure time of 10 s. The average value of microhardness at a point was determined from the results of at least 5 measurements with a confidence level of 95%.

3. Results and discussion

3.1. Macrostructure and microstructure

The macrostructure of the cross section of the consolidated sample containing four layers of CP Ti is shown in Fig. 1. In this figure, the sheet numbers are indicated by Arabic numerals in the order of joining from the bottom to the top, and the joint zones between sheets are indicated by Roman numerals. It can be seen that at a low microscope magnification, welding defects (voids, gaps) are not detected only in joint I, between sheets 1 and 2. In two other joints, II and III, extended voids and gaps are observed (Fig. 1). These defects are often filled with "crumbly" layers of material (Fig. 2), which are probably formed during the deformation of wear particles [16].

A significantly lower quality of joints II and III compared to joint I can be attributed to the appearance of a relief and oxide layer on the surfaces of sheets 2 and 3 contacting with the welding tip during welding. Indeed, both contacting

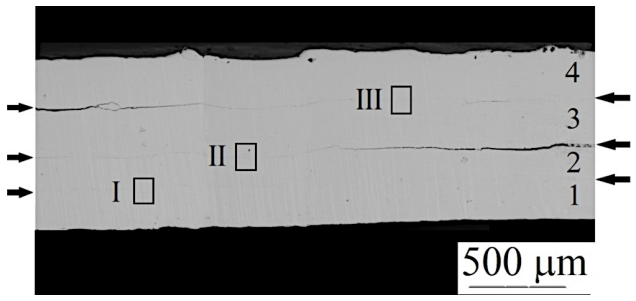

Fig. 1. Macrostructure image of the consolidated sample in the cross section: 1–4 — sheet numbers, I–III — joint zones.

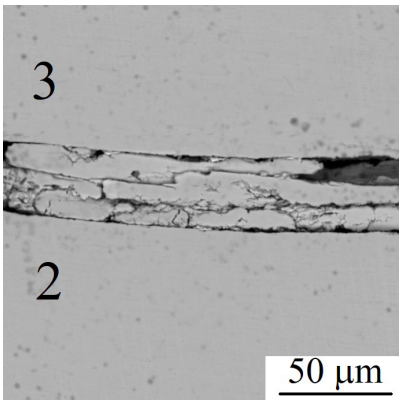

Fig. 2. A gap-like defect between sheets 2 and 3 filled with deformed wear particles.

surfaces of sheets 1 and 2 were smooth and clean due to grinding and washing with isopropyl alcohol before USW. Only a natural oxide layer of several nanometers thick can be present on these surfaces [17,18]. USW of the second sheet was accompanied with a formation of a relief on its upper surface (of no more than 50 μm depth) similar to the relief of the sonotrode tip. This relief is clearly visible on the upper edge of sheet 4 (Fig. 1). In addition, the surface of the weld spot lost its metallic luster and acquired a coating having a light yellow color, which is characteristic of titanium oxide Ti_3O_5 forming at air heating of titanium alloys to the temperature of 300 – 350°C [18]. When joint II was processed, the ground and clean surface of the top sheet 3 was in contact with the textured oxidized surface of bottom sheet 2. A similar situation occurred during the welding of sheet 4. Hence, during USW of sheets 3 and 4 the friction between flat and textured surfaces is accompanied with peeling of materials and the formation of wear particles of titanium. These are deformed under the combination of compression and shear stresses acting during USW partially filling the voids in the joint zone (Fig. 2). It should be noted that a certain level of roughness of the sonotrode surface is necessary for ultrasonic consolidation and is required for the transfer of the mechanical energy from the sonotrode to the sheets, which ensures the bonding in the interface zone during USW [19]. In the present case, however, the formation of even a shallow (weak) relief on the surface of the sheets caused a significant change in the friction conditions and probably led to a sharp decrease in the transmission of vibrations from the welding tip to sheets 3 and 4. Thus, only sheet 2 was maximally involved in the vibration process, which facilitated the achievement of good bonding of the contact surfaces.

Figure 3 shows the BSE images of the microstructure (Fig. 3 a) and crystal orientation maps (Fig. 3 b) obtained from the cross section of the initial sheet and joint zones of the consolidated sample. As one can see from (Fig. 3 a, b), there are no regions of sound bonds in the interface region of joint III. The interface between sheets 3 and 4 has a wavy shape and in its vortices and folds there are clearly visible gaps and pores (Fig. 3 a). In a layer of about 60 μm width around the contact surfaces of sheets 3 and 4, unindexed points predominate in the orientation map (Fig. 3 b). The appearance of such points in EBSD maps may be caused by

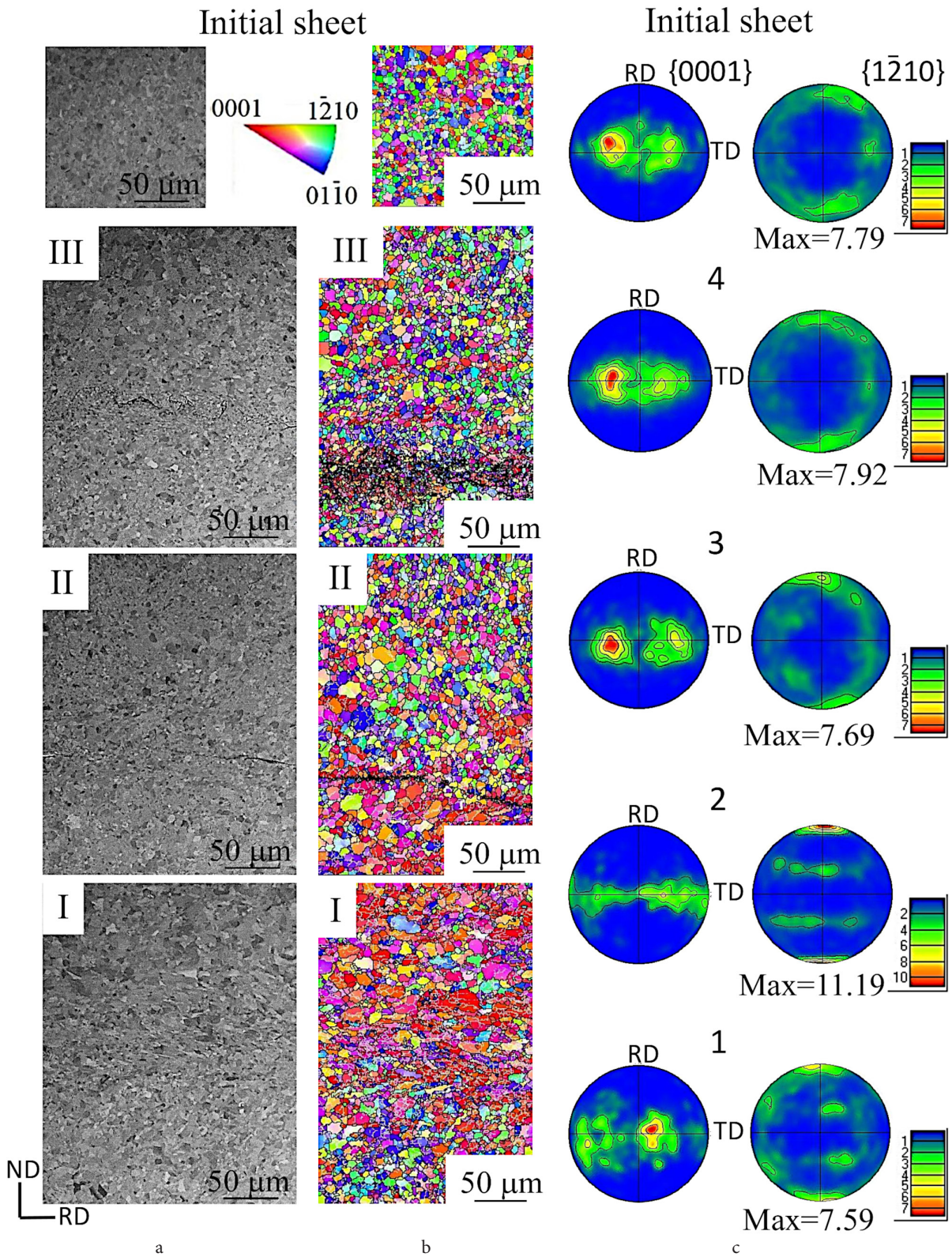

Fig. 3. (Color online) Back-scattered electron images (a) and crystal orientation maps (b) of the cross-sections of initial sheet and weld joints I, II, III; and Pole figures of the initial sheet and welded sheets 1–4 (c). Arabic and Roman numerals correspond to Fig. 1.

the presence of pores and discontinuities (bonding defects) in a material [20]. In joint II (Fig. 3 a, b) alternating bonded and unbonded regions are observed. The interface between sheets 2 and 3 is clearly visible and it has a wavy shape too, but the gaps and pores are located in a layer with the width below 10 mm. Probably, repeated application of the clamping force during sequential welding processes facilitated the filling of voids. No pores and discontinuities are observed in joint I (Fig. 3 a, b) and the contact interface between sheets 1 and 2 completely disappeared. In the weld zone, both small equiaxed grains and larger substructured grains elongated in the direction of vibration of the welding tip are observed.

As was mentioned above, during USC the welding sheets are subjected to high rate oscillating shear strains concentrated near the contact surfaces and to repeated effects of compression and heating. This causes structural evolution not only in the welding zone but also in the bulk of material around (Fig. 3). A comparison of the microstructures (Fig. 3a,b) and microtexture (Fig. 3c) in the sheets 1–4 of the consolidated sample and in the initial sheet shows that the most noticeable changes occurred in sheet 2. After ultrasonic consolidation, a microtexture typical of shear deformation was formed in this sheet [13,21]. In all other sheets (initial one and 1, 3 and 4), the microtexture is similar (Fig. 3c) and it is typical of titanium subjected to sheet rolling [22].

A quantitative microstructural analysis showed that during the consolidation process the average grain size slightly increased and the fraction of LABs enhanced by a factor of approximately 1.5 – 2 in sheets 1 to 4 as compared to the initial one (Fig. 4). The most significant increase of these characteristics was also observed in sheet 2.

The revealed structural differences did not have a significant effect on microhardness of the sheets: the microhardness in the bulk regions of all sheets was about 2000 MPa, whereas the microhardness in the joint zones was 15 – 30% higher (Fig. 5). The increase in the microhardness of joint I was probably associated with the grain-boundary and substructural strengthening. Hardening of joints II and III can be related to the presence of dispersed wear particles, which were observed in gaps between the sheets (Fig. 2).

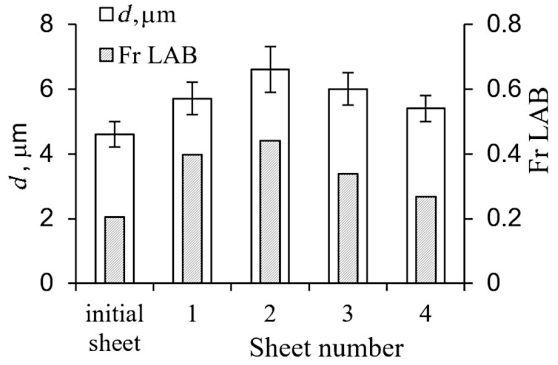

Fig. 4. Average grain size and fraction of LABs in the bulk of titanium sheets before and after ultrasonic consolidation.

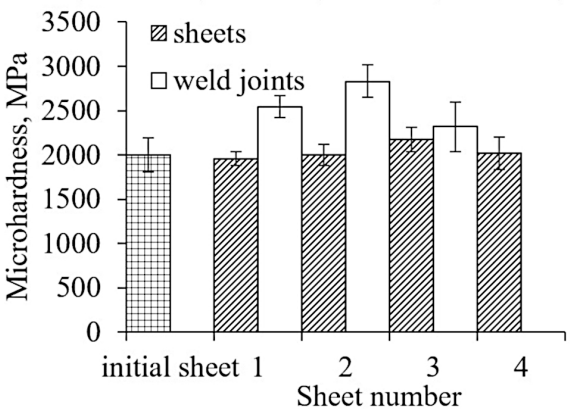

Fig. 5. Change in microhardness over the cross section of a consolidated titanium sample.

4. Conclusions

In the present work, we have made attempt to imitate physically the ultrasonic consolidation process by sequential spot ultrasonic welding and examined the structure and microhardness of a sample obtained by layer-by-layer welding of four sheets of commercially pure titanium.

The results of studies have shown that a welding joint of satisfactory quality was formed only between the first and second sheets. In this joint, microstructure and microtexture typical of shear deformation were formed, which led to an increase in microhardness by approximately 30%. In the bulk of the sheets, weak coarsening of grains and the formation of a subgrain structure were observed. After layer by layer consolidation, the quality of bonding between the sheets decreases from the bottom to the top. This trend indicates that for a material processed by welding of large number of sheets the fraction of sheets with good bonding will increase. Moreover, improvement of the design of welding tip (including its relief and choice of material) and optimization of the welding parameters seem to allow to obtain consolidate titanium samples of better quality.

Acknowledgements. The present work was accomplished in terms of the state assignment of the Institute for Metals Superplasticity Problems of the Russian Academy of Sciences financed by the Ministry of Science and Higher Education of Russia. Electron microscopic studies and mechanical tests were carried out on the facilities of shared services center of IMSP RAS "Structural and Physical-Mechanical Studies of Materials".

References

1. A.K. Gujba, M. Medraj. Advances in Materials Science and Engineering. 2020, 1064870 (2020). Crossref
2. Advances in Manufacturing and Processing of Materials and Structures (ed. by Y. Bar-Cohen). 1st ed. New-York, CRC Press (2018) 560 p. Crossref
3. W.J. Sames, F.A. List, S. Pannala, R.R. Dehoff, S.S. Babu. Int. Mater. Rev. 61 (5), 315 (2016). Crossref
4. B. Dutta, F. H. (Sam) Froes. Metal Powder Report. 72 (2), 96 (2017). Crossref
5. S.M. Thompson, Z.S. Aspin, N. Shamsaei, A. Elwany, L. Bian. Additive Manufacturing. 8, 163 (2015). Crossref
6. R.J. Friel. In: Power Ultrasonics. Applications of High-Intensity Ultrasound (ed. by J.A. Gallego-Juárez, K.F. Graff). Woodhead Publishing (2015) pp. 313 – 335. Crossref
7. P.J. Wolcott, M.J. Dapino. In: Additive Manufacturing Handbook: Product Development for the Defense Industry (ed. by A.B. Badiru, V.V. Valencia, D. Liu). 1st ed. Boca Raton, CRC Press (2017). Crossref
8. C.D. Hopkins, P.J. Wolcott, M.J. Dapino, A.G. Truog, S.S. Babu, S.A. Fernandez. Journal of Engineering Materials and Technology. 134 (1), 011004 (2012). Crossref
9. M.R. Sriraman, S.S. Babu, M. Short. Scripta Materialia. 62, 560 (2010). Crossref
10. P. Wolcott, A. Hehr, M.J. Dapino. Journal of Materials

Research. 29 (17), 2055 (2014). Crossref
11. D. Li. The International Journal of Advanced Manufacturing Technology. 113, 1 (2021). Crossref
12. Z. Zhu, M. Li, Z. Su, D. Zhang, Y. Zhang. In: Transactions on Intelligent Welding Manufacturing (ed. by S. Chen, Y. Zhang, Z. Feng). Singapore, Springer (2018) pp. 120–129.
13. A. A. Mukhametgalina, M. A. Murzinova, A. A. Nazarov. Metall. Mater. Trans. A. 53, 1119 (2022). Crossref
14. E. R. Shayakhmetova, M. A. Murzinova, A. A. Nazarov. Metals. 11 (11), 1800 (2021). Crossref
15. A. A. Mukhametgalina, M. A. Murzinova, A. A. Nazarov. Lett. Mater. 11 (4), 508 (2021). Crossref
16. Jh.-Y. Lin, Sh. Nambu, T. Koseki. ISIJ International. 60 (2), 330 (2020). Crossref
17. U. Zwicker. Titan und titanlegierungen. Springer-Verlag, Berlin (1974) pp. 248 – 337. Crossref
18. Metallovedenie titana i yego splavov (ed. by S. G. Glazunov, B. A. Kolachev). Moscow, Metallurgiya (1992) 352 p. (in Russian)
19. C. Y. Kong, R. C. Soar, P. M. Dickens. Proc. IMechE Pt. C: J. Mech. Eng. Sci. 219, 83 (2005). Crossref
20. F. J. Humphreys. J. Mater. Sci. 36, 3833 (2001). Crossref
21. Y. Jiang, Zh. Chen, C. Zhan, T. Chen, R. Wang, Ch. Liu. Mater. Sci. Eng. A. 640, 436 (2015). Crossref
22. H. Conrad. Prog. Mater. Sci. 26 (2-4), 123 (1981). Crossref